# Mercury transformation and speciation in flue gases from anthropogenic emission sources: A critical review

**L. Zhang[1], S. X. Wang[1,2,*], Q. R. Wu[1], F. Y. Wang[1], C.-J. Lin[3], L. M. Zhang[4], M. L. Hui[1], M. Yang[1], H. T. Su[1], and J. M. Hao[1,2]**

[1] State Key Joint Laboratory of Environment Simulation and Pollution Control, School of Environment, Tsinghua University, Beijing 100084, China

[2] State Environmental Protection Key Laboratory of Sources and Control of Air Pollution Complex, Beijing 100084, China

[3] Center for Advances in Water and Air Quality, Lamar University, Beaumont, TX, USA

[4] Air Quality Research Division, Science and Technology Branch, Environment Canada, Toronto, Canada

*Correspondence to:* S. X. Wang (shxwang@tsinghua.edu.cn)

**Abstract.** Mercury transformation mechanisms and speciation profiles are reviewed for mercury formed in and released from flue gases of coal-fired boilers, non-ferrous metal smelters, cement plants, iron and steel plants, municipal solid waste incinerators, and biomass burning. Mercury in coal, ores and other raw materials is released to flue gases in the form of $Hg^0$ during combustion or smelting in boilers, kilns or furnaces. Decreasing temperature from over 800°C to below 300°C in flue gases leaving boilers, kilns or furnaces promotes homogeneous and heterogeneous oxidation of gaseous elemental mercury ($Hg^0$) to gaseous divalent mercury ($Hg^{2+}$), with a portion of $Hg^{2+}$ adsorbed onto fly ash to form particulate-bound mercury ($Hg_p$). Halogen is the primary oxidizer for $Hg^0$ in flue gases, and active components (e.g., $TiO_2$, $Fe_2O_3$, etc.) on fly ash promote heterogeneous oxidation and adsorption processes. In addition to mercury removal, mercury transformation also occurs when passing through air pollution control devices (APCDs), affecting the mercury speciation in flue gases. In coal-fired power plants, selective catalytic reduction (SCR) system promotes mercury oxidation by 34–

85%, electrostatic precipitator (ESP) and fabric filter (FF) remove over 99% of $Hg_p$, and wet flue gas desulfurization system (WFGD) captures 60–95% of $Hg^{2+}$. In non-ferrous metal smelters, most $Hg^0$ is converted to $Hg^{2+}$ and removed in acid plants (APs). For cement clinker production, mercury cycling and operational conditions promote heterogeneous mercury oxidation and adsorption. The mercury speciation profiles in flue gases emitted to the atmosphere are determined by transformation mechanisms and mercury removal efficiencies by various APCDs. For all the sectors reviewed in this study, $Hg_p$ accounts for less than 5% in flue gases. In China, mercury emission has a higher $Hg^0$ fraction (66–82% of total mercury) in flue gases from coal combustion, in contrast to a greater $Hg^{2+}$ fraction (29–90%) from non-ferrous metal smelting, cement and iron/steel production. The higher $Hg^{2+}$ fractions shown here than previous estimates may imply stronger local environmental impacts than previously thought, caused by mercury emissions in East Asia. Future research should focus on determining mercury speciation in flue gases from iron and steel plants, waste incineration and biomass burning, and on elucidating the mechanisms of mercury oxidation and adsorption in flue gases.

## 1 Introduction

Atmospheric mercury is one of the key focuses in the global environmental issues in recent years owing to its toxicity, persistence and long-range transportability. The international treaty on mercury, the Minamata Convention, was adopted worldwide in October 2013 aiming to reduce mercury release into the immediate environments. Coal combustion, cement clinker production, and primary production of ferrous and non-ferrous metals, are predominant sources of global anthropogenic mercury emission (UNEP, 2013a). Aside from coal-fired power plants, coal-fired industrial boilers, cement clinker production facilities, and smelting and roasting processes used in the production of non-ferrous metals (lead, zinc, copper and industrial gold), waste incineration facilities, in terms of their rapid growth, are also on the list of key point sources in Annex D for Article 8 of the Minamata Convention (UNEP, 2013b).

Mercury has three major chemical forms: gaseous elemental mercury ($Hg^0$), gaseous oxidized (or reactive) mercury ($Hg^{2+}$) and particulate-bound mercury ($Hg_p$). $Hg^0$, the most stable form, accounts for over 90% of the total mercury in the atmosphere. Its residence time is estimated to be several months to over one year (Schroeder and Munthe, 1998; Lindberg et al., 2007; Fu et al., 2012), but could be as short as hours to weeks under specific environmental conditions (Gustin et al., 2008). $Hg^{2+}$ has high water-solubility and thus can be easily scavenged into droplets and adsorbed to surfaces followed by wet and dry deposition. The short residence time (hours to days) of $Hg^{2+}$leads to more prominent local environmental impacts. $Hg_p$ has a residence time of hours to weeks, and mercury on finer particles can be transported for long distances (Schroeder and Munthe, 1998). $Hg^{2+}$ and $Hg_p$ are also referred to as reactive mercury (RM) due to their high surface reactivity (Rutter and Schauer, 2007). Mercury speciation profiles in the exhausted flue gases from key sources determine the behavior of atmospheric mercury in the ambient air, while the profiles in the pipeline flue gases are crucial to mercury emission controls.

Different emission sources have different mercury speciation profiles. Even for the same emission category, the profile varies significantly when different combinations of air pollution control devices (APCDs) are applied or different types of fuels or raw materials are used. Different countries or regions have distinguished mercury speciation profiles for similar emission sources because of APCD preferences and fuel (or raw material) properties. The profiles can vary with time as advanced air pollution control technologies are implemented. Inventory experts tend to use more localized and up-to-date profiles from on-site measurements of mercury emission sources. Walcek et al. (2003) employed three sets of profiles respectively for fuel combustion, waste incineration and other manufacturing processes, and found the overall relative emission proportions (REPs) among $Hg^0$:$Hg^{2+}$:$Hg_p$ species for the 1996 inventory of eastern North America to be 47:35:18. Streets et al. (2005) accomplished a more detailed profile list for different source categories with profiles under different APCDs for coal combustion, and obtained the overall REPs for China in 1999 which were 56:32:12. Pacyna et al. (2006) developed the 2000 mercury emission inventory for Europe and

evaluated the overall REPs to be 61:32:7. The REPs for anthropogenic mercury emissions from Korea in 2007 were estimated to be 64:29:7 (Kim et al., 2010a), and those for the 2006 inventory of Australia were 77:17:6 (Nelson et al., 2012). Our recent study updated the anthropogenic mercury emission inventory of China to the calendar year 2010 based on an abundant database of field measurements, and the REPs of the overall mercury speciation profile were 58:39:3 (Zhang et al., 2015). Although the ratio of $Hg^0$ to $Hg^{2+}$ seems to be close to the results from Streets et al. (2005), the sectoral profiles have changed significantly because of the implementation of APCDs in key sources in China. Results from on-site measurements in Chinese power plants, non-ferrous metal smelters and cement plants have substantially improved the speciation profiles.

Mercury speciation profiles of major emission sources in the world have remarkable influences on the assessment of long-range transport of atmospheric mercury. This paper provides a critical review of mercury speciation in flue gases from major anthropogenic emission sources, and elaborates the process of initial mercury release in boilers, kilns or furnaces to its transformation in the flue gases across APCDs. Key factors during the emission process for each source are identified for the enhancement of existing control technologies. Profiles of mercury speciation in different countries and regions are compared by sectors to assess their local and regional environmental impacts.

## 2 Mercury speciation and transformation in flue gases from coal combustion

### 2.1 Mercury speciation in flue gas from coal combustion

Nearly all mercury in coal is released into the flue gas in the form of $Hg^0$ during combustion over 1000°C. With the decrease of flue gas temperature out of the boiler, a portion of $Hg^0$ is oxidized to $Hg^{2+}$ mainly by active atomic Cl generated from HCl, $Cl_2$ or HOCl (Senior et al., 2000). Niksa et al. (2001) discovered that the cycling of atomic Cl is the dominant mechanism of $Hg^0$ oxidation. This process, including homogeneous and heterogeneous reactions, is driven by thermodynamic equilibrium, but restricted by reaction kinetics (Widmer et al., 2000). Based on the results from bench-scale

experiments, L. Zhang et al. (2013a) found that lower total mercury concentration and higher chlorine concentration in flue gas lead to higher $Hg^0$ oxidation rate. The results from Sterling et al. (2004) showed that $SO_2$ and NO in flue gas inhibit the oxidation of $Hg^0$. The homogeneous reaction mechanism usually underestimates the oxidation rate because heterogeneous reactions on fly ash play a more important role under low temperatures (100°C to 300°C). Heterogeneous processes not only accelerate the oxidation of $Hg^0$ but also contribute to the adsorption of $Hg^{2+}$ onto fly ash to form $Hg_p$. Bhardwaj et al. (2009) found that specific surface area (SSA), loss on ignition (LOI) and average particle size positively correlated with both the $Hg^0$ oxidation and the $Hg^{2+}$ adsorption. Inorganic components such as CuO, $TiO_2$ and $Fe_2O_3$ also have significant impacts on the mercury oxidation and adsorption processes (Dunham et al., 2003; Norton et al., 2003; López-Antón et al., 2007).

According to 30 previous on-site measurements in coal-fired power plants and industrial boilers (Kellie et al., 2004; Duan et al., 2005; Lee et al., 2006; Zhou et al., 2006; Chen et al., 2007; Yang et al., 2007; Chen et al., 2008; Wang et al., 2008; Zhou et al., 2008; Kim et al., 2010b; Wang et al., 2010a; Zhang et al., 2012a; L. Zhang et al., 2013a), mercury speciation after the boiler and before APCDs is mainly determined by coal properties, specifically chlorine, mercury and ash contents in coal. Chlorine and mercury contents have the most significant impacts on the percentage of $Hg^{2+}$ in total mercury, while mercury and ash contents highly influence the proportion of $Hg_p$ in total mercury in flue gas. The proportions of $Hg^0$, $Hg^{2+}$ and $Hg_p$ in the flue gas released from a pulverized-coal (PC) boiler, averaged 56%, 34% and 10%, respectively. However, $Hg^{2+}$ proportion ranged from 5% to 82% while $Hg_p$ proportion ranged from 1% to 28%. Besides the coal properties, the boiler type also affects mercury speciation in flue gas. A circulating fluidized bed (CFB) boiler can generate as high as 65% of $Hg_p$ in flue gas due to more sufficient contact between gaseous phase mercury and fly ash inside the boiler (Zhang, 2012).

## 2.2 Mercury transformation across APCDs for coal combustion

### 2.2.1 Mercury transformation during selective catalytic reduction (SCR)

Figure 1 shows mercury transformation and removal processes across APCDs in coal-fired power plants. The first APCD after the boiler could be the SCR system if applied for $NO_x$ control. The operation temperature in a SCR is typically 300–400°C. SCR catalysts, usually composed of $V_2O_5$, $WO_3$ and $TiO_2$, significantly promote the $Hg^0$ oxidation process and increase $Hg^{2+}$ level for downstream removal in PM and $SO_2$ control devices (Niksa and Fujiwara, 2005). Laboratory-scale studies (Lee et al., 2003; Bock et al., 2003) showed that $Hg^0$ oxidant inside SCR is the atomic Cl. The Hg-Cl redox chemistry and the NO-$NH_3$ redox chemistry occur simultaneously on the active sites of SCR catalyst (L. Zhang et al., 2013b). Therefore, the reaction system in SCR is complicated and influenced by a number of factors. Machalek et al. (2003) pulled subbituminous-derived flue gas into a pilot-scale SCR system and found that the $Hg^0$ oxidation extent decreased from 40% to 5% when the space velocity (SV) of SCR was increased from 3000 to 7800 $hr^{-1}$. The influence of $NH_3$ is more controversial. The study of Machalek et al. (2003) found that $NH_3$ inhibits the oxidation of $Hg^0$ inside SCR. Niksa and Fujiwara (2005) theoretically calculated this process and addressed the inhibition mechanism by $NH_3$ competing with atomic Cl on active sites. However, on-site measurements in three coal-fired power plants showed the opposite results, that is, the increase of $NH_3$ injection rate promotes $Hg^0$ oxidation (L. Zhang et al., 2013b). Possible chemical mechanism was proposed for the observed oxidation, but requires further investigation. The concentrations of NO, $SO_2$ and total mercury and the type and on-duty time of the SCR catalyst also affect the heterogeneous oxidation processes inside SCR (Winberg et al., 2004; Niksa and Fujiwara, 2005; L. Zhang et al., 2013b). Field tests in coal-fired power plants showed an average $Hg^0$ oxidation rate of 71% with a range of 34–85% (Chen et al., 2008; Zhang, 2012; L. Zhang et al., 2013b).

### 2.2.2 Mercury transformation in electrostatic precipitator (ESP)

Due to its high PM removal efficiency and relatively low cost, ESP is the most widely used PM controller in coal-fired power plants. Over 99% of $Hg_p$ is removed inside ESP (Wang et al., 2010a). A small portion of $Hg^{2+}$ can also be adsorbed onto fly ash and removed by ESP. The $Hg^{2+}$ capture rate is determined by the unburned carbon (UBC)

on fly ash (Senior and Johnson, 2005). The total mercury removal efficiency of ESP is usually in the range of 20–40% at ~5% UBC content of fly ash. Besides the UBC, the surface property, size, porous structure and mineral composition of fly ash affect the mercury capture rate of ESP as well (Lu et al., 2007). When coal with high chlorine content is burned, more UBC is generated on fly ash and more $Hg^{2+}$ and $Hg_p$ are formed in flue gas, which in turn increase the mercury capture rate inside ESP. Improvement of ESP for capturing fine particles (e.g., adding electric fields inside ESP) will also increase mercury removal efficiency. Inter-conversion between $Hg^0$ and $Hg^{2+}$ occurs inside ESP (Zhang, 2012). The charging anode of ESP can neutralize $Hg^{2+}$ and convert it to $Hg^0$, while $Hg^0$ in flue gas continues to be oxidized to $Hg^{2+}$ via heterogeneous reactions in ESP under temperatures of 150–200°C. Therefore, $Hg^0$ concentration can either increase or decrease inside ESP depending on the processes interplay. On-site measurements showed an average mercury removal efficiency of 29% for ESP with a large range of 1–74% (Goodarzi, 2004; Guo et al., 2004; Kellie et al., 2004; Tang, 2004; Duan et al., 2005; Lee et al., 2006; Chen et al., 2007; Yang et al., 2007; Wang et al., 2008; Zhou et al., 2008; Kim et al., 2010b; Shah et al., 2010; ICR, 2010; Wang et al., 2010a; Zhang et al., 2012a). Nevertheless, ESP installed after a CFB boiler can achieve an average of 74% mercury removal due to the high $Hg_p$ proportion in flue gas (Chen et al., 2007; ICR, 2010; Zhang, 2012).

### 2.2.3 Mercury transformation in fabric filter (FF)

A higher PM removal efficiency can be achieved by FF than by ESP, especially for fine particles. FF is increasingly applied in coal-fired power plants and industrial boilers in the need of fine particle ($PM_{2.5}$ or $PM_1$) control. FF has mercury removal efficiencies of 9–92% with an average of 67% (Chen et al., 2007; Shah et al., 2008; Wang et al., 2009; ICR, 2010). Besides $Hg_p$, FF can also remove over 50% of $Hg^{2+}$. During the filtration, contact between flue gas and the particles on the cake layer promotes adsorption of $Hg^{2+}$ onto fly ash (Zhang, 2012). The properties of fly ash have the most significant impact on $Hg^{2+}$ adsorption. The dust cake layer can also facilitates the oxidation of $Hg^0$ (Wang et al., 2016a).

Some plants apply ESP-FF hybrid precipitator to improve the fine particle removal efficiency. Limited studies suggested an overall mercury removal rate of 39% in ESP-FF hybrid precipitator (S. X. Wang et al., 2014).

### 2.2.4 Mercury transformation during wet flue gas desulfurization (WFGD)

WFGD is the most widely used APCD for $SO_2$ control in coal-fired power plants. During sulfur (mainly $SO_2$) scrubbing process, $Hg^{2+}$ is also removed in WFGD. The average mercury removal efficiency of WFGD is 64%, ranging from 56% to 88% (Lee et al., 2006; Chen et al., 2007; Kim et al., 2010b; Wang et al., 2010a). Insoluble $Hg^0$ passes through WFGD without being captured. Chemical reduction of the dissolved $Hg^{2+}$ reduces total mercury removal efficiency in WFGD due to re-volatilization of $Hg^0$ (Wo et al., 2009; Ochoa-González et al., 2013). Flue gas and slurry composition, operating temperature, limestone injection rate, and slurry pH are the key factors affecting the re-volatilization of $Hg^0$ (Acuña-Caro et al., 2009; Ochoa-González et al., 2012; Schuetze et al., 2012). WFGD is the crucial step in the co-benefit mercury control technologies in coal-fired power plants. The applications of high-chlorine coal, SCR and halogen addition can increase the $Hg^{2+}$ proportion in flue gas before WFGD, which will enhance the overall mercury capture efficiency of WFGD. Therefore, the optimized strategy for WFGD is to stabilize the $Hg^{2+}$ in the WFGD slurry to prevent mercury re-volatilization. The overall mercury removal efficiency of WFGD is on average 45% with a range of 10–85% (Yokoyama et al., 2000; Kilgroe et al., 2002; Ito et al., 2006; Lee et al., 2006; Meij and Winkel, 2006; Chen et al., 2007; Kim et al., 2010b; Wang et al., 2010a).

### 2.2.5 Mercury transformation in wet scrubber (WS)

Coal-fired industrial boilers are usually in a smaller scale compared with the utility boilers. The PM control for industrial boilers are not as advanced as those for power plants in developing countries. For example, WS is most widely adopted in China's industrial boilers. The proportion of $Hg_p$ in flue gas of industrial boilers (1–3%) is not as high as that of power plants because of the shorter formation times of $Hg_p$ in

industrial boilers, especially in small-scale ones. Consequently, the $Hg_p$ removal rate of WS is only about 50% (Zhang, 2012). $SO_2$ in flue gas can dissolve in water and form $SO_3^{2-}$, which could be a reducing agent for $Hg^{2+}$, leading to low $Hg^{2+}$ capture rates in WS (Chang and Ghorishi, 2003; Omine et al., 2012). The overall mercury removal rate of WS is 23% on average with a range of 7–59% (Zhang, 2012).

### 2.3 Mercury speciation profile for coal-fired boilers

Mercury speciation profiles in the flue gas from coal combustion are summarized in Table 1, which considers the transformation of mercury species across different types of APCDs (Goodarzi, 2004; Guo et al., 2004; Kellie et al., 2004; Tang, 2004; Duan et al., 2005; Lee et al., 2006; Zhou et al., 2006; Chen et al., 2007; Yang et al., 2007; Chen et al., 2008; Shah et al., 2008; Wang et al., 2008; Zhou et al., 2008; Kim et al., 2010b; Shah et al., 2010; Wang et al., 2010a; Zhang, 2012; Zhang et al., 2012a; L. Zhang et al., 2013b). When no APCD is applied, mercury speciation profile has the largest variability due to the different properties of coal burned. The average proportions of $Hg_p$ are all below 2% when PM control devices are installed. As commonly used for stoker-fired (SF) industrial boilers, WS removes a large proportion of $Hg_p$ and a small proportion of $Hg^{2+}$, resulting in a decrease of $Hg_p$ percentage and a slight increase of $Hg^0$ percentage compared with the case of non-control. The average percentages of $Hg^0$ and $Hg^{2+}$ in the flue gas exhausted from ESP are 58% and 41%, respectively. The presence of CFB boiler can increase the proportion of $Hg^0$. The proportions of $Hg^0$ and $Hg^{2+}$ are similar in the flue gas after FF, although with large variability. For the combination of ESP+WFGD, the proportion of $Hg^0$ reaches as high as 84%. With the existence of SCR, the average proportion of $Hg^0$ is not as high as that for the combination of ESP+WFGD because of the high oxidation rate of $Hg^0$ inside SCR. Large uncertainties still exist in flue gas from the combinations of PC+FF, PC+FF+WFGD and CFB+ESP, since scarce speciation data is available.

## 3 Mercury speciation and transformation in flue gases from non-ferrous metal smelters

### 3.1 Mercury speciation in the roasting/smelting furnaces

Non-ferrous metals (zinc, lead, copper and industrial gold) are mainly produced from sulfide ores. Usually, mercury is released from concentrates to flue gases during the pyrometallurgical processes of non-ferrous metals. A typical pyrometallurgical process requires four stages, including dehydration, smelting/roasting, extraction, and refining (Wang et al., 2010b; Zhang et al., 2012b; Wu et al., 2015). Approximately 1% of mercury in concentrates is released to flue gas in the dehydration kiln, where the temperature varies from 150–700°C (Song, 2010). Mercury in concentrates is mainly released during smelting/roasting stage. The temperatures in the smelting/roasting, thermal extraction and thermal refining stages are all higher than 800°C (Li et al., 2010; Wang et al., 2010b). The Hg-S and Hg-O bonds are broken under such high temperatures (Hylander and Herbert, 2008). Almost all mercury compounds are thermally dissociated into $Hg^0$ considering the thermodynamic stability of $Hg^0$ at this temperature (Wang, 2011). Mercury release rates during these stages are generally over 98% (Song, 2010; Li et al., 2010; Wu et al., 2015). The case in the industrial gold smelting process is an exception. Based on our on-site measurements, only 85% of the mercury in gold concentrate evaporates into the flue gas with the roasting temperature at 600°C (Yang, 2015). The low mercury release rate in the tested gold smelter may be related to chemical properties of mercury and gold. According to a previous study (Li, 1990), mercury at certain chemical speciation in gold ores only releases when the temperature exceeds 780°C. The released $Hg^0$ would be transformed to $Hg^{2+}$ or $Hg_p$ by catalytic oxidation in the flue gas with the existence of gas phase oxidants such as atomic Cl (Galbreath and Zygarlicke, 2000; L. Zhang et al., 2013a).

### 3.2 Mercury transformation across APCDs for the roasting/smelting flue gas

Flue gases from the four stages typically go through dust collectors to remove particles. FF or ESP is generally adopted for flue gases from the dehydration, extraction and refining stages, whereas a combination of waste heat boiler, cyclone and ESP is used for the roasting/smelting flue gas (Wu et al., 2012; UNECE, 2013). The flue gas is then cleaned in a purification system including flue gas scrubber (FGS) and

electrostatic demister (ESD) before entering the acid plant for $SO_2$ recovery (see Fig. 2). To minimize heavy metal emissions, the roasting/smelting flue gas could also require additional mercury removal after the purification system (UNECE, 2013). Since the roasting/smelting stage releases the most mercury, previous studies focus on mercury transformation and removal inside APCDs for the roasting/smelting flue gas (Zhang et al., 2012b; Wu et al., 2015). Figure 3 shows the mercury speciation after APCDs for non-ferrous metal smelters. Overall, the $Hg_p$ proportion is less than 5% for all non-ferrous metal smelters. $Hg^0$ is the dominant species in the flue gas after the purification devices in most situation since most $Hg^{2+}$ has been removed. However, when the flue gas goes through the acid plant, the share of $Hg^{2+}$ increases to 80-98%.

### 3.2.1 Mercury transformation in the dust collectors

Dust collectors can remove >99% of particles and therefore $Hg_p$ is mostly removed simultaneously. $Hg_p$ proportion after dust collectors is less than 5% (Zhang et al., 2012b; Wu et al., 2015). $Hg^0$ can be homogeneously or heterogeneously oxidized in the flue gas, while the charging anode in the ESP can reduce $Hg^{2+}$ to $Hg^0$. Therefore, the resulting mercury speciation profile after the dust collectors depends on the competition between $Hg^{2+}$ reduction and $Hg^0$ oxidation. The proportion of $Hg^{2+}$ after dust collectors varies a lot (4–85%) among different tested smelters (Zhang et al., 2012b; Wu et al., 2015). The total mercury removal efficiency of dust collectors is usually less than 20%. Test results of three zinc smelters showed mercury removal efficiencies of 9–12% (Wu et al., 2015). The study of Li et al. (2010) shows lower mercury removal efficiencies of dust collectors (1–5%). ESP plays the most important role in mercury removal for roasting/smelting flue gas. Zhang et al. (2012b) found an average mercury removal rate of 12%, which is much lower than the efficiency of ESPs in coal-fired power plants, because of two reasons. Firstly, higher temperature of ESPs in smelters (300–350°C compared to more or less 150°C in coal-fired power plants) would restrain the $Hg^0$ condensation and $Hg^{2+}$ absorption processes (Meij and Winkel, 2006). Secondly, although the dust concentrations in the flue gases of the coal-fired power plants and the non-ferrous metal smelters are at the same level, mercury concentration in flue gas of

316 non-ferrous metal smelters is two to three orders higher than that in the flue gas of coal-
317 fired power plants (Tang et al., 2007; Wang et al., 2010a,b; Zhang, 2012; Zhang et al.,
318 2012a,b; Wu et al., 2015). Under such conditions, there might not be sufficient active
319 sites on the particles for mercury adsorption in the flue gas of non-ferrous metal
320 smelters.

321 **3.2.2 Mercury transformation in purification systems**

322 The purification system generally includes FGS and ESD. Unlike WS or WFGD for
323 $SO_2$ control in coal combustion, FGS in non-ferrous metal smelters uses diluted sulfuric
324 acid to capture $SO_2$ and $SO_3$. The yield from FGS is waste acid, which will be treated
325 to acid sludge. ESD is employed to remove water vapor from flue gas. Li et al. (2010)
326 and Wang et al. (2010b) found that mercury removal efficiency in FGS was 11–22%,
327 whereas ESD removed 10–42% of total mercury in the flue gas. The overall mercury
328 removal efficiency of the purification systems in six tested plants by Zhang et al. (2012b)
329 varies in the range of 72–99%. Studies of Zhang et al. (2012b) and Kim et al. (2011)
330 show that higher $Hg^{2+}$ in the flue gas entering the purification system leads to higher
331 mercury removal efficiency considering the high solubility of $Hg^{2+}$ in water and sulfuric
332 acid. In addition, $Hg^0$ would condense to liquid metallic mercury when the temperature
333 of flue gas decreases from 300°C to approximately 25°C at the outlet of the purification
334 system (Song, 2010). Previous studies have observed liquid $Hg^0$ in the removed waste
335 acid (Wang, 2011). The dominant mercury species after the purification system is
336 generally $Hg^0$, with a proportion 43–96% (Wang et al., 2010b; Zhang et al., 2012b; Wu
337 et al., 2015).

338 **3.2.3 Mercury transformation in other mercury removal systems**

339 Mercury in the flue gas can be removed by other techniques including Boliden-
340 Norzink process, Bolchem process, Outokumpu process, sodium thiocyanate process,
341 selenium scrubber, activated carbon filters, and selenium filter (UNECE, 2013). The
342 removal mechanisms in these processes are either to oxidize $Hg^0$ into $Hg^{2+}$or $Hg^+$ with
343 strong oxidants and then remove oxidized mercury, or to capture $Hg^0$ with specific

adsorbents. The Boliden-Norzink process, the most widely used process in non-ferrous metal smelters, has been installed in more than 40 smelters globally. On-site measurements indicated that its mercury removal efficiency is 83–92% (Wang et al., 2010b; Li et al., 2010; Wu et al., 2015). In the Boliden-Norzink process, $Hg^0$ in the flue gas is oxidized to $Hg_2Cl_2$ by solution containing $HgCl_2$. The yield $Hg_2Cl_2$ is removed from the circulating solution and then either used for mercury production or stored, whereas the solution is reused after regeneration. Other processes are not as commercialized as the Boliden-Norzink process.

### 3.2.4 Mercury transformation in the acid plants

An acid plant generally includes dehydration tower, conversion tower and absorption tower. Dehydration tower uses 93–95% sulfuric acid to remove the water vapor. Conversion tower converts $SO_2$ into $SO_3$ with vanadium catalysts. Absorption tower absorbs $SO_2$ with 98% sulfuric acid. Tests in one zinc smelter with a mercury reclaiming tower indicates that mercury speciation profile ($Hg^0$:$Hg^{2+}$:$Hg_p$) after the acid plant is 6:90:4 (Wang et al., 2010b). Wu et al. (2015) found that the proportion of $Hg^{2+}$ increased from 4% to 98% when passing the acid plant. The total mercury removal efficiency in the acid plant can reach 83%. On-site measurements in six smelters by Zhang et al. (2012b) showed that the dominant species was $Hg^{2+}$ after the acid plant with the double-conversion-double-absorption process, while $Hg^0$ became the dominant species after the single-conversion-single-absorption process. The net reaction of mercury in the acid plant is the oxidation of $Hg^0$, either by the oxidants in flue gas under the vanadium catalysts in the conversion tower or by the concentrated sulfuric acid. However, further studies are required to understand the oxidation mechanisms.

## 3.3 Mercury speciation profile for non-ferrous metal smelters

Mercury speciation profiles in the flue gases from non-ferrous metal smelters are summarized in Table 2. In early mercury emission inventories, the relative emission proportions (REPs) among $Hg^0$:$Hg^{2+}$:$Hg_p$ species for non-ferrous metal smelters were estimated to be 80:15:5 (Pacyna and Pacyna, 2002; Streets et al., 2005; Pacyna et al.,

2006; Wu et al., 2006). However, recent field tests found that the proportion of $Hg^{2+}$ could reach >90% for the smelting/roasting stage with acid plants (Wang et al., 2010b; Zhang et al., 2012b). Besides the smelting/roasting stage, mercury emissions from the slag dehydration and volatilization stages are also significant. According to field experiments in a zinc smelter (Wang et al., 2010b), the mercury emissions from these two stages were 95 g/d and 50 g/d, respectively, even higher than that from the roasting process (22 g/d). Therefore, the overall mercury speciation profile for non-ferrous metal smelters is not only affected by the roasting/smelting flue gases but also by the dehydration flue gas and the volatilization flue gas. Mass flow analysis in three zinc smelters indicates that mercury emissions from the slag dehydration stage, the slag smelting stage and the volatilization stage accounted for 54–98% of total emissions, with $Hg^0$ as the dominant form (Wu et al., 2015). When considering atmospheric mercury emissions from all thermal processes in addition to the roasting process, the emission proportion of $Hg^{2+}$ is reduced to 29–51% (Wu et al., 2015). In lead smelters, the proportion of $Hg^{2+}$ is about 40% when considering atmospheric mercury emissions from the extracting and reclaiming processes (Zhang et al., 2012b). The proportion of $Hg^{2+}$ in all exhausted gases is 32–68% in copper smelters with the double-conversion-double-absorption process installed for the roasting flue gas (Zhang et al., 2012b). The mercury speciation profile ($Hg^0$:$Hg^{2+}$:$Hg_p$) in the exhausted flue gases in gold smelters with the double-conversion-double-absorption process is estimated to be 32:57:11 (Yang, 2015).

# 4 Mercury speciation and transformation in flue gas from cement clinker production

## 4.1 Cement clinker production processes

A mix of raw materials, mainly limestone, are heated up to over 1400°C and different compositions react to produce clinker. Additives, usually gypsum, are then mixed with clinker and milled to produce cement. The temperature of the final cement production is usually under 100°C. Results from temperature programmed decomposition (TPD) experiments indicate that mercury is not released from gypsum at such temperatures

401 (Rallo et al., 2010; López-Antón et al., 2011; Liu et al., 2013). Therefore, we only
402 consider the clinker production process that includes shaft kilns, wet rotary kilns, dry
403 rotary kilns and precalciner processes.
404 Precalciner process is usually composed of the raw mill system, the coal mill system,
405 the kiln system and the kiln head system. Raw materials are ground and homogenized
406 in the raw mill system. The fuel, usually coal, is prepared in the coal mill system
407 including coal mill and FF. The kiln system for the production of cement clinker
408 includes the preheater, the precalciner and the rotary kiln. The prepared raw materials,
409 namely raw meal, enter the kiln system from one end of rotary kiln (kiln tail), and the
410 coal powder is brought into the kiln system by air from the other kiln end (kiln head).
411 The solid materials flow in opposite direction with the flue gas. The flue gas from kiln
412 tail is used to preheat raw materials in raw mill and coal in coal mill. The flue gas from
413 kiln head is de-dusted and then emitted into the atmosphere. All the dust collected by
414 dust collector is recycled to kiln system.

415 **4.2 Mercury behavior in cement clinker production process**

416 The mercury behavior in cement production process is summarized as three stages:
417 vaporization, adsorption and recycling (Sikkema et al., 2011) (see Fig. 4). At the
418 vaporization stage, mercury in raw materials and fuel is vaporized into flue gas in the
419 kiln system. Then part of the mercury in flue gas is captured by raw materials in the
420 raw mill and coal in the coal mill when the flue gas is used to preheat solid materials,
421 and part of the mercury in flue gas is also collected in the dust collector with dust. This
422 process is called the adsorption stage. Finally, the mercury is cycled back into the kiln
423 system with raw materials, coal and collected dust, which is the recycling stage.
424 Therefore, there are three mercury cycles in the precalciner clinker production process.
425 Mercury cycling in cement plants has been confirmed in field tests (Mlakar et al., 2010;
426 Paone, 2010; Sikkema et al., 2011; Zheng et al., 2012). A transient model was
427 developed to simulate mercury concentration in flue gas from kiln tail (Senior et al.,
428 2010). This model was based on a series of mass balances from preheater to the whole
429 process.

The three mercury cycles cause mercury enrichment in the clinker production process. F. Y. Wang et al. (2014) assessed mercury enrichment process using the ratio of mercury concentration in the exhausted flue gas to the equivalent mercury concentration. The equivalent mercury concentration was defined by dividing the total mercury input from raw materials and coal with the total amount of flue gas emerged in the kiln system. It was found that the mercury concentration was enriched by as high as 4–15 times in two Chinese cement plants. Another study also confirmed this point, with the mercury concentration enriched by over 10 times (Mlakar et al., 2010).

Mercury enrichment can affect its emission from cement plants. The cement clinker production process has two modes depending on the operation of raw mill. When the raw mill is on (operation mode), the flue gas flows through raw mill first and then emitted into the atmosphere after dust removal. When the raw mill is off (direct mode), the flue gas directly flows through the FF after the raw mill and emits into the atmosphere. In operation mode, a larger proportion of mercury in flue gas is recirculated and enriched in the system because the combination of raw mill and FF has a higher mercury removal efficiency than FF alone. Therefore, switching between the two modes significantly changes mercury enrichment and concentration in flue gas. It should be noted that mercury concentration in the clinker is low. If no filtered dust is discarded, over 90% of mercury input from raw materials and coal is eventually emitted into the atmosphere (Paone, 2008; Linero, 2011; Hoenig and Zunzer, 2013).

### 4.3 Mercury transformation during cement clinker production process

In mercury vaporization stage, mercury in raw materials and coal is released into the flue gas. Field tests in power plants of previous studies indicated that almost all of the mercury in coal (>99%) was vaporized into the flue gas as the elementary form because of the high temperature in coal-fired boilers, which is usually higher than 1000°C (Tang et al., 2007; Wang et al., 2010a; Zhang et al., 2012a). For the cement clinker production process, mercury in raw materials and coal is mostly released to the flue gas. Mercury concentration in clinker was less than 5 ng/g, accounting for only 1.9–6.1% of the total mercury (F. Y. Wang et al., 2014). The compounds of mercury silicates might be the

459 main chemical forms of mercury in clinker (Schreiber et al., 2005). Temperature of raw
460 materials increases continuously from 400°C at the inlet of the preheater to over 1400°C
461 in the rotary kiln. Different mercury species have different decomposition and boiling
462 temperatures, as summarized in one previous study (Zheng et al., 2012). Further studies
463 on identification of mercury species in raw meals are needed to understand the
464 mechanism of mercury vaporization in kiln system.

465 Mercury is oxidized homogeneously and heterogeneously in flue gas. As analyzed
466 by F. Y. Wang et al. (2014), a series of operational conditions in the cement clinker
467 production process can promote mercury oxidation. The oxidation of mercury is usually
468 kinetically limited (Senior et al., 2000; Niksa et al., 2001; Wilcox et al., 2003;
469 Krishnakumar and Helble, 2007; Liu et al., 2010). Residence time over 20 s provides
470 enough reaction time for mercury oxidation. The high concentration of PM in flue gas,
471 usually over 10 g/m$^3$, can catalyze the oxidation; and the addition of Fe-containing
472 material in raw materials can provide more active sites for heterogeneous mercury
473 oxidation (Dunham et al., 2003; Galbreath et al., 2005; Bhardwaj et al., 2009).
474 Vaporized $Hg^0$ in the kiln system is oxidized during the cooling process of flue gas.
475 Considering that $Hg^{2+}$ can be easily adsorbed onto the surface of PM in flue gas and the
476 PM concentration in flue gas is high, the proportion of $Hg_p$ is therefore high. Mercury
477 speciation in the flue gas entering the raw mill system was measured in three cement
478 plants (F. Y. Wang et al., 2014). The proportion of $Hg^{2+}$ was in the range of 64–76%,
479 while the proportion of $Hg_p$ was 21–27%. Mlakar et al. (2010) found that the proportion
480 of $Hg_p$ in another plant was even higher, ranging in 15–77%. The high proportion of
481 $Hg^{2+}$ and $Hg_p$ can cause a high mercury removal efficiency in APCDs and other
482 facilities, including dust collectors, raw mill and coal mill. Mercury removal
483 efficiencies of raw mill with FF and coal mill with FF could reach 86–89% and 94–
484 95%, respectively (F. Y. Wang et al., 2014). The mechanisms of mercury removal in
485 raw mill and FF are different. The removal of $Hg_p$ in FF and adsorption of $Hg^{2+}$ onto
486 the filter cake are considered to be the predominant mechanism in FF (Chen et al., 2007;
487 Wang et al., 2010a). At mercury recycling stage, the removed mercury in raw mill, coal
488 mill and dust collectors is eventually cycled into kiln system with raw mill, coal powder

and dust, respectively. Overall, because of the existing mercury cycling and a series of operational conditions promoting mercury oxidation, mercury speciation during clinker production is dominated by $Hg^{2+}$ and $Hg_p$.

### 4.4 Mercury speciation profile for cement plants

The mercury emissions from the cement clinker production process were previously considered to be composed of 80% $Hg^0$, 15% $Hg^{2+}$ and 5% $Hg_p$ (Streets et al., 2005). Recent field results (Mlakar et al., 2010; Won and Lee, 2012; F. Y. Wang et al., 2014) on mercury emission speciation of cement production are shown in Table 3. The proportions of different mercury species fluctuate at a wide range. Won and Lee (2012) found that $Hg^{2+}$ only accounted for 15% of the total mercury emissions, while other studies (VDZ, 2002; Mlakar et al., 2010; Linero, 2011; F. Y. Wang et al., 2014) showed that $Hg^{2+}$ was the dominant species accounting for 60% to >90% of the total mercury. As discussed above, the mercury speciation and emission are largely variable because of the complicated mercury cycling and operational modes of the cement clinker production process. Previous estimates of mercury emission and speciation from cement clinker production have large uncertainties. More studies including field tests should be conducted to further understand the mechanism of mercury speciation and transformation in cement production.

## 5 Mercury speciation and transformation in flue gases from other emission sources

In this section, the behavior of mercury in flue gases from other emission sources, including iron and steel production, waste incineration, biomass burning, cremation, and PVC production, are introduced. Although there are still other mercury emission sources not discussed in this study, such as oil combustion, few field measurements are available for mercury speciation and transformation inside these sources.

### 5.1 Mercury speciation and transformation in flue gas from iron and steel production

Iron and steel production is composed of raw material preparation (rotary kilns for

limestone and dolomite production and the coking process), sintering machine, blast furnace and convertor. In raw material preparation, limestone and dolomite are roasted in rotary kilns and coking coal is produced in coke oven. Iron ores, coke and limestone (dolomite) are then mixed and roasted in the sintering machine, namely the sintering process. Products of these two stages are fed to the blast furnace where sinter, coke and limestone are smelted to produce iron, and then the iron is smelted in a convertor to produce steel. There is also another process using steel scrap to produce steel, called electric furnace. To increase the utilization efficiency of energy, coal gas emerged in the coke oven, blast furnace and convertor is collected and burned to generate electricity. The operational conditions in different stages are quite different. The mercury behavior in iron and steel plants is therefore quite complicated.

Mercury is vaporized in high-temperature facilities, including coke oven, sintering machine, blast furnace and convertor. Mercury in the flue gas is oxidized homogeneously and heterogeneously. Part of the mercury is removed in dust collectors and flue gas desulfurization devices, and the remaining mercury in flue gas is emitted into the atmosphere. Field tests indicated that the mercury release rates in coke oven and sintering machine were lower than that in coal-fired boilers (>99%) because of the lower temperature in these facilities (Wang et al., 2016b). Previous studies indicated that the mercury emissions from sintering machine accounted for about 90% of total emissions from iron and steel plants (Fukuda et al., 2011). A speciation profile of 80% $Hg^0$, 15% $Hg^{2+}$ and 5% $Hg_p$ was applied in Streets et al. (2005). However, oxidized mercury was found to be the predominant species in our recent study (Wang et al., 2016b). The proportion of $Hg^{2+}$ in flue gas reached as high as 59–73% and the proportion of $Hg_p$ was under the detection limit because of the installation of ESPs for the examined iron and steel plants (Wang et al., 2016b). The high PM concentration in flue gas and Fe on PM could promote mercury oxidation in flue gas. More field tests need to be conducted on mercury speciation profile of this industry in the future.

### 5.2 Mercury speciation and transformation in flue gas from waste incineration

Waste incineration is a potential predominant source in the global mercury emission

546 inventory. The major incineration types are municipal solid waste (MSW) incineration,
547 medical waste incineration and industrial/hazardous waste incineration. A significant
548 proportion of mercury (80–96%) in the MSW releases from the incinerator into the flue
549 gas is in the form of $Hg^0$ at 850–1000°C (Park et al., 2008). Grate furnace combustor
550 (GFC) and circulation fluidized bed combustor (CFBC) are the two most commonly
551 used incinerators. The flue gas from CFBC has a larger proportion of $Hg_p$ than that from
552 GFC. Typical APCDs for incinerators are combinations of semi-dry or dry flue gas
553 deacidification (SD-FGD or D-FGD) for $SO_2$ and HCl removal and dust controller (e.g.,
554 WS+ESP, FF, FF+WS, etc.). SCR is sometimes used as well for $NO_x$ control. Activated
555 carbon injection (ACI) is used for the control of persistent organic pollutants (POPs),
556 which is required for incinerators in China.
557 The overall mercury removal efficiency of the APCDs for MSW incineration ranges
558 from 60% to over 99% (Zhang et al., 2008; Takahashi et al., 2012). Previous studies in
559 Europe and the USA indicated that the $Hg^{2+}$ proportion in the exhausted flue gas
560 ranges from 75% to 85%(Pacyna and Münch, 1991; Carpi, 1997). A Korean study found
561 the $Hg^{2+}$ proportion in MSW incinerators to be in the range of 78–89%, and that in
562 industrial waste incinerators are even as high as 96.3–98.7% (Park et al., 2008). Kim et
563 al. (2010a) tested two medical waste incinerators with SD-FGD+FF+WS and got the
564 $Hg^0$ proportion to be 43.9% and 96.8% respectively. A Japanese study showed that an
565 industrial waste incinerator with WS and wet ESP has the $Hg^0$ proportion of 92.7%
566 (Takahashi et al., 2012). Based on field measurements in eight MSW incinerators in
567 China, Chen et al. (2013) found that average $Hg^{2+}$ proportion in flue gas from the outlet
568 of GFC+SD-FGD+ACI+FF is 96%, while that for CFBC+SD-FGD+ACI+FF is 64%.
569 High chlorine content in the waste results in high $Hg^{2+}$ proportion in the flue gas.
570 Limestone slurry or powder sprayed in SD-FGD or D-FGD absorbs a large amount of
571 $Hg^{2+}$ and activated carbon adsorbs a large amount of both $Hg^0$ and $Hg^{2+}$. Particles from
572 SD-FGD and ACI are captured by the downstream FF. $Hg_p$ is removed by all types of
573 dust controllers. The high $Hg^{2+}$ formation rate due to the oxidative condition in flue gas
574 and the high $Hg^{2+}$ removal rate by APCDs (especially SD-FGD, FF and ACI) cause the
575 significant variation in mercury speciation profiles for incinerators.

### 5.3 Mercury speciation and transformation in flue gas from biomass burning

Biomass burning mainly includes biomass fuel burning and open biomass burning. Biomass fuel can be divided into fuel woods, crop residues and biomass pellets. Usually, there is no APCD for biomass burning. Huang et al. (2011) tested four different types of wood fuels and found the $Hg^0$ proportion to be 95–99% and the rest is basically $Hg^{2+}$. Wei (2012) found that $Hg^0$ in flue gas from biomass burning is 70–90% of total mercury while that of $Hg^{2+}$ ranges from 5% to 9%. $Hg_p$ proportion differs a lot between different biomass fuel types: 12%, 25% and 1% for fuel wood, crop residues and biomass pellets, respectively. Hu et al. (2012) differentiated the emission factors for biomass burning and cooking/space heating in rural areas to be 0.035 and 0.515 g Hg/t biomass burned, respectively. W. Zhang et al. (2013) tested 25 types of fuel wood, 8 types of crop residues and 2 types of biomass pellets, and found that the mercury emission rate during biomass burning is 78–99% while the remainder stays in the residue. The mercury speciation profile (ratio of $Hg^0$, $Hg^{2+}$ and $Hg_p$ to total Hg) for fuel wood was 76%, 6% and 18%, and that for crop residue was similar (73%, 4% and 23%). However, the speciation profile for biomass pellets is quite different. Due to the more complete combustion, $Hg^0$ accounts for as high as 97% in the flue gas from of biomass pellets combustion. W. Zhang et al. (2013) calculated mercury emission from biomass burning in China and gave the shares of $Hg^0$, $Hg^{2+}$ and $Hg_p$ at 74%, 5% and 21%, respectively. Open biomass burning generally involves forest wildfires, grassland/savanna wildfires, and agriculture residue burning. Friedli et al. (2003) investigated the mercury speciation from burning of temperate North American forests through both laboratory and airborne measurements. Their research showed that the dominant species is $Hg^0$, accounting for 87–99% of the total mercury, and the rest is mainly $Hg_p$.

### 5.4 Mercury speciation and transformation in flue gas from cremation

Researches on mercury speciation and transformation in flue gas from cremation are very limited. Takaoka et al. (2010) conducted field measurements in seven crematories in Japan, two of them without any APCDs, one with ESP and four with FF for particle control. Advanced APCDs such as catalytic reactor and activated carbon filter are

605 installed in three of the tested crematories. In the exhausted flue gases, $Hg^0$ is averagely
606 the dominant mercury species but with significant variation (25–99%). Extremely large
607 uncertainties exist in this sector due to the large diversity of mercury content in human
608 body and whether the dental amalgam is applied.

609 ### 5.5 Mercury speciation and transformation in flue gas from PVC production

610 Aside from combustion and some high-temperature industrial processes, there are
611 some other processes with intentional mercury use that also have mercury emissions.
612 The production of polyvinyl chloride (PVC) with the calcium carbide process utilizes
613 a catalyst containing large amounts of mercury. Ren et al. (2014) conducted on-site
614 measurements in a PVC production line and found that 71.5% of the total mercury was
615 lost from the catalyst, most of which was recovered by the mercury remover, accounting
616 for 46% of the total mercury. The total mercury emitted to the atmosphere only
617 accounted for less than 1% of the total mercury in the catalyst. The speciation tests
618 indicated that most of the mercury escaped from the catalyst was $Hg^0$, as no $Hg^{2+}$ was
619 detected virtually.

620 ## 6 Comparison of mercury speciation profiles in different countries and regions

621 Table 4 summarizes the sectoral mercury speciation profiles in different countries
622 and regions (Pacyna et al., 2006; AMAP/UNEP, 2008; Chrystall and Rumsby, 2009;
623 Kim et al., 2010a; Lin et al., 2012; Nelson et al., 2012; Zhang et al., 2015). China and
624 South Korea have compiled extensive speciation profiles based on observational data
625 collected at anthropogenic mercury emission sources. The inventories for Europe and
626 New Zealand used same speciation data as the global inventory for coal combustion,
627 which is close to the results of South Korea. China has different speciation data for coal
628 combustion, where the proportion of $Hg^0$ is higher than that reported in other countries.
629 This is probably because the high WFGD installation rate in China results in higher
630 $Hg^{2+}$ removal efficiency. Mercury speciation for coal-fired power plants, industrial and
631 residential coal combustion are also different. Residential coal combustion has the
632 lowest $Hg^{2+}$ proportion while industrial coal combustion has the highest. This is mainly

influenced by the boiler type and the APCDs applied. Residential stove has a short temperature-decrease time, which reduces formation of $Hg^{2+}$. The APCDs applied for industrial coal combustion have a lower $Hg^{2+}$ removal efficiency than those applied for coal-fired power plants.

Global inventory applied similar speciation profiles for most other industrial sectors, i.e., 80% $Hg^0$, 15% $Hg^{2+}$ and 5% $Hg_p$. The inventories estimated in China and South Korea provide speciation profiles for different sectors. The sectors of non-ferrous metal smelting (including zinc, lead and copper), cement production and iron and steel production in China have higher $Hg^{2+}$ proportions than most of the other countries, which is caused by catalytic mercury oxidation in acid plants in non-ferrous metal smelters and the intensive heterogeneous mercury oxidation in cement plants and steel plants. The higher $Hg^{2+}$ proportions imply that mercury emission from East Asia could have more local environmental impacts than previously expected. Our recent study (L. Wang et al., 2014) indicated that anthropogenic sources in China contribute 35–50% of the total mercury concentration and 50–70% of the total deposition in polluted regions in China.

## 7 Conclusions

The initial speciation of mercury after the boiler, smelter or kiln varies significantly because of the diverse qualities of coals or raw materials. Nearly all mercury in coal is released into the flue gas in the form of $Hg^0$ during combustion. $Hg^0$ is the predominant mercury species in exiting flue gases from coal-fired power plants mainly due to the high $Hg_p$ removal efficiency of ESP or FF and the high $Hg^{2+}$ removal efficiency of WS or WFGD. The enhancement of $Hg^0$ oxidation in SCR and by halogen injection is effective for mercury emission control in coal-fired power plants. outlet of On the contrary, $Hg^{2+}$ tends to be the principal form in the flue gases emitted from non-ferrous metal smelters, cement plants and iron and steel plants. Catalytic metallic components and high PM concentrations in flue gases are the two primary causes. Flue gas purification systems and processes in acid plants for non-ferrous metal smelting contribute to the largest amount of mercury removal in non-ferrous metal smelters.

Specific mercury reclaiming tower in non-ferrous metal smelters preferentially releases $Hg^0$ to downstream flue gases. The key to mercury emission controls in cement plants is to break the mercury cycling processes during the dust recirculation for the kiln, raw mill and coal mill. Since $Hg^{2+}$ dominates the mercury speciation of emissions from cement plants and iron and steel plants, WS or WFGD could be implemented for mercury abatement.

Mercury speciation profiles for key sources reported in recent studies are significantly different from those obtained in early studies. This is partially because the APCDs used in these sources have advanced in the past two decades. Another reason lies in the lack of on-site measurements in early emission estimates where certain speciation profiles were assumed. Adoption of different APCDs and use of different fuels or raw materials cause distinct differences found in mercury speciation profiles applied in different countries or regions. Large proportion of $Hg^{2+}$ from non-ferrous metal smelters, cement plants and iron and steel plants calls for local attention. There are still large uncertainties in the speciation profiles at key sources, such as iron and steel plants, waste incineration and biomass burning. More on-site measurements for these sources should be carried out to complete the database of mercury emission speciation. Research is also needed in understanding the mechanism of mercury oxidation and adsorption in flue gases with different compositions, which benefits mercury emission controls. Accurate speciation profiles improve the performance of regional transport and dispersion models to better assess the environmental impacts of mercury emissions into the atmosphere.

*Acknowledgment.* This work was funded by Major State Basic Research Development Program of China (973 Program) (No. 2013CB430001 and No. 2013CB430003) and National Natural Science Foundation of China (No. 21307070).

## References

Acuña-Caro, C., Brechtel, K., Scheffknecht, G., and Braß, M.: The effect of chlorine and oxygen concentrations on the removal of mercury at an FGD-batch reactor,

692 Fuel, 88, 2489–2494, 2009.
693 Arctic Monitoring and Assessment Programme (AMAP) and United Nations
694 Environment Programme (UNEP): Technical Background Report to the Global
695 Atmospheric Mercury Assessment, Geneva, Switzerland, 2008.
696 Bhardwaj, R., Chen, X. H., and Vidic, R. D.: Impact of fly ash composition on mercury
697 speciation in simulated flue gas, J. Air Waste Manage., 59, 1331–1338, 2009.
698 Bock, J., Hocquel, M. J. T., Unterberger, S., and Hein, K. R. G.: Mercury oxidation
699 across SCR catalysts of flue gas with varying HCl concentrations, U.S.
700 Environmental Protection Agency-Department of Energy-EPRI Combined
701 Power Plant Air Pollutant Control Symposium, 19–20 May 2003, Washington,
702 DC, USA, 2003.
703 Carpi, A.: Mercury from combustion sources: a review of the chemical species emitted
704 and their transport in the atmosphere, Water, Air and Soil Pollution, 98, 241–254,
705 1997.
706 Chang, J. S., and Ghorishi, S. B.: Simulation and evaluation of elemental mercury
707 concentration increase in flue gas across a wet scrubber, Environ. Sci. Technol.,
708 37, 5763–5766, 2003.
709 Chen, L., Duan, Y., Zhuo, Y., Yang, L., Zhang, L., Yang, X., Yao, Q., Jiang, Y., and Xu,
710 X.: Mercury transformation across particulate control devices in six power plants
711 of China: The co-effect of chlorine and ash composition, Fuel, 86(4), 603–610,
712 2007.
713 Chen, J., Yuan, D., Li, Q., Zheng, J., Zhu, Y., Hua, X., He, S., and Zhou, J.: Effect of
714 flue-gas cleaning devices on mercury emission from coal-fired boiler, P. CSEE,
715 28(2), 72–76, 2008.
716 Chen, L. G., Liu, M., Fan, R. F., Ma, S. X., Xu, Z. C., Ren, M. Z., and He, Q. S.:
717 Mercury speciation and emission from municipal solid waste incinerators in the
718 Pearl River Delta, South China, Sci. Total Environ., 447, 396–402, 2013.
719 Chrystall, L., and Rumsby, A.: Mercury Inventory for New Zealand 2008, available at:
720 http://www.mfe.govt.nz/sites/default/files/mercury-inventory-new-zealand-
721 2008.pdf (last access: 23 November 2015), 2009.

722 Duan, Y., Cao, Y., Kellie, S., Liu, K., Riley, J. T., and Pan, W.: In-situ measurement and
723 distribution of flue gas mercury for a utility PC boiler system, J. Southeast Univ.,
724 21(1), 53–57, 2005.
725 Dunham, G. E., Dewall, R. A., and Senior, C. L.: Fixed-bed studies of the interactions
726 between mercury and coal combustion fly ash, Fuel Process. Technol., 82(2–3),
727 197–213, 2003.
728 Friedli, H. R., Radke, L. F., Lu, J. Y., Banic, C. M., Leaitch, W. R., and MacPherson, J.
729 I.: Mercury emissions from burning of biomass from temperate North American
730 forests:laboratory and airborne measurements, Atmos. Environ., 37, 253–267,
731 2003.
732 Fu, X. W., Feng, X. B., Sommar, J., and Wang, S. F.: A review of studies on atmospheric
733 mercury in China, Sci. Total Environ., 421–422, 73–81, 2012.
734 Fukuda, N., Takaoka, M., Doumoto, S., Oshita, K., Morisawa, S., and Mizuno, T.:
735 Mercury emission and behavior in primary ferrous metal production, Atmos.
736 Environ., 45(22), 3685–3691, 2011.
737 Galbreath, K. C., and Zygarlicke, C. J.: Mercury transformations in coal combustion
738 flue gas, Fuel Process. Technol., 65–66, 289–310, 2000.
739 Galbreath, K. C., Zygarlicke, C. J., Tibbetts, J. E., Schulz, R. L., and Dunham, G. E.:
740 Effects of NOx, α-Fe2O3, γ-Fe2O3, and HCl on mercury transformations in a 7-
741 kW coal combustion system, Fuel Process. Technol., 86, 429–448, 2005.
742 Goodarzi, F.: Speciation and mass-balance of mercury from pulverized coal fired power
743 plants burning western Canadian subbituminous coals, J. Environ. Monit., 6(10),
744 792–798, 2004.
745 Guo, X., Zheng, C., Jia, X., Lin, Z., and Liu, Y.: Study on mercury speciation in
746 pulverized coal-fired flue gas, P. CSEE, 24(6), 185–188, 2004.
747 Gustin, M. S., Lindberg, S. E., and Weisberg, P. J.: An update on the natural sources
748 and sinks of atmospheric mercury, Appl. Geochem., 23, 482–493, 2008.
749 Hoenig, V. H. R., and Zunzer, U.: Guidance document on BAT-BEP for mercury in the
750 cement industry, Technical report of the European Cement Research Academy
751 (ECRA) on behalf of WBCSD Cement Sustainability Initiative, TR-ECRA

0049a/2013/M, available at: http://www.unep.org/chemicalsandwaste/Portals/9/CSI_Hg-Report_final_10_06_13.pdf (last access: 23 November 2015), 2013.

Hu, D., Zhang, W., Chen, L., Chen, C., Ou, L. B., Tong, Y. D., Wei, W., Long, W. J., and Wang, X. J.: Mercury emissions from waste combustion in China from 2004 to 2010, Atmos. Environ., 62, 359–366, 2012.

Huang, J. Y., Hopke, P. K., Choi, H.-D., Laing, J. R., Cui, H. L., Zananski, T. J., Chandrasekaran, S. R., Rattigan, O. V., and Holsen, T. M.: Mercury (Hg) emissions from domestic biomass combustion for space heating, Chemosphere, 84, 1694–1699, 2011.

Hylander, L. D., and Herbert, R. B.: Global emission and production of mercury during the pyrometallurgical extraction of nonferrous sulfide ores, Environ. Sci. Technol., 42(16), 5971–5977, 2008.

Information Collection Request (ICR): Results from onsite measurements in USA, Washington, DC, USA, 2010.

Ito, S., Yokoyama, T., and Asakura, K.: Emissions of mercury and other trace elements from coal-fired power plants in Japan, Sci. Total Environ., 368(1), 397–402, 2006.

Kellie, S., Duan, Y., Cao, Y., Chu, P., Mehta, A., Carty, R., Liu, K., Pan, W., and Riley, J. T.: Mercury emissions from a 100-MW wall-fired boiler as measured by semicontinuous mercury monitor and Ontario Hydro Method, Fuel Process. Technol., 85(6–7), 487–499, 2004.

Kilgroe, J., Sedman, C., Srivastava, R., Ryan, J., Lee, C., and Thorneloe, S.: Control of mercury emissions from coal-fired electric utility boilers: interim report including errata dated 3-21-02, EPA-600/R-01-109, EPA Office of Research and Development, National Risk Management and Research Laboratory: Research Triangle Park, NC, USA, 2002.

Kim, J. H., Park, J. M., Lee, S. B., Pudasainee, D., and Seo, Y. C.: Anthropogenic mercury emission inventory with emission factors and total emission in Korea, Atmos. Environ., 44, 2714–2721, 2010a.

Kim, J. H., Pudasainee, D., Yoon, Y. S., Son, S. U., and Seo, Y. C.: Studies on speciation

changes and mass distribution of mercury in a bituminous coal-fired power plant by combining field data and chemical equilibrium calculation, Ind. Eng. Chem. Res., 49, 5197–5203, 2010b.

Kim, J. H., Pudasainee, D., Jung, S. J., and Seo, Y. C.: Speciation and mass balance of mercury in non-ferrous metals manufacturing facilities, The 10th International Conference on Mercury as a Global Pollutant, 24–29 July 2011, Halifax, Nova Scotia, Canada, 2011.

Krishnakumar, B., and Helble, J. J.: Understanding mercury transformations in coal-fired power plants: Evaluation of homogeneous Hg oxidation mechanisms, Environ. Sci. Technol., 41, 7870–7875, 2007.

Lee, C. W., Srivastava, R. K., Ghorishi, S. B., Hastings, T. W., and Stevens, F. M.: Study of speciation of mercury under simulated SCR NOx emission control conditions, U.S. Environmental Protection Agency-Department of Energy-EPRI Combined Power Plant Air Pollutant Control Symposium, 19–20 May 2003, Washington, DC, USA, 2003.

Lee, S. J., Seo, Y. C., Jang, H. N., Park, K. S., Baek, J. I., An, H. S., and Song, K. C.: Speciation and mass distribution of mercury in a bituminous coal-fired power plant, Atmos. Environ., 40(12), 2215–2224, 2006.

Li, G. H., Feng, X. B., Li, Z. G., Qiu, G. L., Shang, L. H., Liang, P., Wang, D. Y., and Yang, Y. K.: Mercury emission to atmosphere from primary Zn production in China, Sci. Total Environ., 408(20), 4607–4612, 2010.

Li, J.: Distribution features of mercury compounds in gold deposits, Geology and Exploration, 11, 46–51, 1990.

Lin, C. J., Shetty, S. K., Pan, L., Pongprueksa, P., Jang, C., and Chu, H. W.: Source attribution for mercury deposition in the contiguous United States: Regional difference and seasonal variation, J. Air Waste Manage., 62(1), 52–63, 2012.

Lindberg, S. E., Bullock, R., Ebinghaus, R., Engstrom, D., Feng, X. B., Fitzgerald, W., Pirrone, N., Prestbo, E., and Seigneur, C.: A synthesis of progress and uncertainties in attributing the sources of mercury in deposition, Ambio, 36, 19–32, 2007.

812 Linero, A. A.: Synopsis of mercury controls at Florida cement plants, The 104th Annual
813 Conference and Exhibition of the Air and Waste Management Association, 21–
814 24 June 2011, Orlando, Florida, USA, 2011.
815 Liu, J., Qu, W., Yuan, J., Wang, S., Qiu, J., and Zheng, C.: Theoretical studies of
816 properties and reactions involving mercury species present in combustion flue
817 gases, Energ. Fuel., 24, 117–122, 2010.
818 Liu, X. L., Wang, S. X., Zhang, L., Wu, Y., Duan, L., and Hao, J. M.: Speciation of
819 mercury in FGD gypsum and mercury emission during the wallboard production
820 in China, Fuel, 111, 621–627, 2013.
821 López-Antón, M. A., Díaz-Somoano, M., Abad-Valle, P., and Martínez-Tarazona, M.
822 R.: Mercury and selenium retention in fly ashes: Influence of unburned particle
823 content, Fuel, 86, 2064–2070, 2007.
824 López-Antón, M. A., Perry, R., Abad-Valle, P., Díaz-Somoano, M., Martínez-Tarazona,
825 M. R., and Maroto-Valer, M. M.: Speciation of mercury in fly ashes by
826 temperature programmed decomposition, Fuel Process. Technol., 92, 707–711,
827 2011.
828 Lu, Y., Rostam-Abadi, M., Chang, R., Richardson, C., and Paradis, J.: Characteristics
829 of fly ashes from full-scale coal-fired power plants and their relationship to
830 mercury adsorption, Energ. Fuel., 21, 2112–2120, 2007.
831 Machalek, T., Ramavajjala, M., Richardson, M., and Richardson, C.: Pilot evaluation
832 of flue gas mercury reactions across an SCR unit, U.S. Environmental Protection
833 Agency-Department of Energy-EPRI Combined Power Plant Air Pollutant
834 Control Symposium, 19–20 May 2003, Washington, DC, USA, 2003.
835 Meij, R., and Winkel, H. t.: Mercury emissions from coal-fired power stations: The
836 current state of the art in the Netherlands, Sci. Total Environ., 368(1), 393–396,
837 2006.
838 Mlakar, T. L., Horvat, M., Vuk, T., Stergaršek, A., Kotnik, J., Tratnik, J., and Fajon, V.:
839 Mercury species, mass flows and processes in a cement plant, Fuel, 89(8), 1936–
840 1945, 2010.
841 Nelson, P. F., Morrison, A. L., Malfroy, H. J., Cope, M., Lee, S., Hibberd, M. L., Meyer,

842 C. P., and McGregor, J.: Atmospheric mercury emissions in Australia from
843 anthropogenic, natural and recycled sources, Atmos. Environ., 62, 291–302,
844 2012.
845 Niksa, S., Helble, J. J., and Fujiwara, N.: Kinetic modeling of homogeneous mercury
846 oxidation: The importance of NO and H2O in predicting oxidation in coal-
847 derived systems, Environ. Sci. Technol., 35, 3701–3706, 2001.
848 Niksa, S., and Fujiwara, N.: A predictive mechanism for mercury oxidation on selective
849 catalytic reduction catalysts under coal-derived flue gas, J. Air Waste Manage.,
850 55(12), 1866–1875, 2005.
851 Norton, G. A., Yang, H., Brown, R. C., Laudal, D. L., Dunham, D. E., and Erjavec, J.:
852 Heterogeneous oxidation of mercury in simulated post combustion conditions,
853 Fuel, 82, 107–116, 2003.
854 Ochoa-González, R., Díaz-Somoano, M., López-Antón, M. A., and Martínez-Tarazona,
855 M. R.: Effect of adding aluminum salts to wet FGD systems upon the stabilization
856 of mercury, Fuel, 96, 568–571, 2012.
857 Ochoa-González, R., Díaz-Somoano, M., and Martínez-Tarazona, M. R.: Influence of
858 limestone characteristics on mercury re-emission in WFGD systems, Environ.
859 Sci. Technol., 47, 2974–2981, 2013.
860 Omine, N., Romero, C. E., Kikkawa, H., Wu, S., and Eswaran, S.: Study of elemental
861 mercury re-emission in a simulated wet scrubber, Fuel, 91, 93–101, 2012.
862 Pacyna, E. G., and Pacyna, J. M.: Global emission of mercury from anthropogenic
863 sources in 1995, Water, Air and Soil Pollution, 137, 149–165, 2002.
864 Pacyna, E. G., Pacyna, J. M., Steenhuisen, F., and Wilson, S.: Global anthropogenic
865 mercury emission inventory for 2000, Atmos. Environ., 22(40), 4048–4063, 2006.
866 Pacyna, J. M., and Münch, J.: Anthropogenic mercury emission in Europe, Water, Air
867 and Soil Pollution, 56, 51–61, 1991.
868 Paone, P.: Mercury controls for the cement industry, Cement Industry Technical
869 Conference, 28 March–1 April 2010, Colorado Springs, Colorado, USA, 2010.
870 Park, K. S., Seo, Y. C., Lee, S. J., and Lee, J. H.: Emission and speciation of mercury
871 from various combustion sources, Powder Technol., 180, 151–156, 2008.

872 Rallo, M., López-Antón, M. A., Perry, R., and Maroto-Valer, M. M.: Mercury speciation
873 in gypsums produced from flue gas desulfurization by temperature programmed
874 decomposition, Fuel, 89, 2157–2159, 2010.
875 Ren, W., Duan, L., Zhu, Z. W., Du, W., An, Z. Y., Xu, L. J., Zhang, C., Zhuo, Y. Q., and
876 Chen, C. H.: Mercury transformation and distribution across a polyvinyl chloride
877 (PVC) production line in China, Environ. Sci. Technol., 48(4), 2321–2327, 2014.
878 Rutter, A. P., and Schauer, J. J.: The effect of temperature on the gas – particle
879 partitioning of reactive mercury in atmospheric aerosols, Atmos. Environ.,
880 41(38), 8647–8657, 2007.
881 Schreiber, R. J., Kellet, C. D., Joshi, N., and Skokie, I. L.: Inherent mercury controls
882 within the Portland cement kiln system, Portland Cement Association, Skokie, IL,
883 USA, 2005.
884 Schroeder, W. H., and Munthe, J.: Atmospheric mercury - An overview, Atmos.
885 Environ., 32(5), 809–822, 1998.
886 Schuetze, J., Kunth, D., Weissbach, S., and Koeser, H.: Mercury vapor pressure of flue
887 gas desulfurization scrubber suspensions: effects of the pH level, gypsum and
888 iron, Environ. Sci. Technol., 46, 3008–3013, 2012.
889 Senior, C. L., Sarofim, A. F., Zeng, T., Helble, J. J., and Mamani-Paco, R.: Gas-phase
890 transformations of mercury in coal-fired power plants, Fuel Process. Technol., 63,
891 197–213, 2000.
892 Senior, C., and Johnson, S.: Impact of carbon-in-ash on mercury removal across
893 particulate control devices in coal-fired power plants, Energ. Fuel., 19, 859–863,
894 2005.
895 Senior, C., Montgomery, C. J., and Sarofim, A.: Transient model for behavior of
896 mercury in Portland cement kilns, Ind. Eng. Chem. Res., 49, 1436–1443, 2010.
897 Shah, P., Strezov, V., Prince, K., and Nelson, P. F.: Speciation of As, Cr, Se and Hg
898 under coal fired power station conditions, Fuel, 87(10–11), 1859–1869, 2008.
899 Shah, P., Strezov, V., and Nelson, P.: Speciation of mercury in coal-fired power station
900 flue gas, Energ. Fuel., 24, 205–212, 2010.
901 Sikkema, J. K., Alleman, J. E., Ong, S. K., and Wheelock, T. D.: Mercury regulation,

902 fate, transport, transformation, and abatement within cement manufacturing
903 facilities: review, Sci. Total Environ., 409(20), 4167–4178, 2011.
904 Song, J. X.: Study on atmospheric mercury emissions from typical zinc smelting
905 process, M.S. thesis, Tsinghua University, Beijing, China, 2010.
906 Sterling, R. O., Qiu, J. R., and Helble, J. J.: Experimental study of mercury
907 homogeneous reaction chemistry under post-flame conditions, The 227th Spring
908 ACS National Meeting, 28 March–1 April 2004, Anaheim, CA, USA, 2004.
909 Streets, D. G., Hao, J. M., Wu, Y., Jiang, J. K., Chan, M., Tian, H. Z., and Feng, X. B.:
910 Anthropogenic mercury emissions in China, Atmos. Environ., 39(40), 7789–
911 7806, 2005.
912 Takahashi, F., Shimaoka, T., and Kida, A.: Atmospheric mercury emissions from waste
913 combustions measured by continuous monitoring devices, J. Air Waste Manage.,
914 62(6), 686–695, 2012.
915 Takaoka, M., Oshita, K., Takeda, N., and Morisawa, S.: Mercury emission from
916 crematories in Japan, Atmos. Chem. Phys., 10, 3665–3671, 2010.
917 Tang, S.: The mercury species and emissions from coal combustion flue gas and landfill
918 gas in Guiyang, Ph.D. thesis, Institute of Geochemistry, Chinese Academy of
919 Sciences, Guiyang, China, 2004.
920 Tang, S. L., Feng, X. B., Qiu, J. R., Yin, G. X., and Yang, Z. C.: Mercury speciation and
921 emissions from coal combustion in Guiyang, southwest China, Environ. Res.,
922 105(2), 175–182, 2007.
923 United Nations Economic Commission for Europe (UNECE): Guidance document on
924 best available techniques for controlling emissions of heavy metals and their
925 compounds from the source categories listed in annex II to the Protocol on Heavy
926 Metals, Geneva, Switzerland, 2013.
927 United Nations Environment Programme (UNEP): Global Mercury Assessment 2013:
928 Sources, Emissions, Releases and Environmental Transport, Geneva,
929 Switzerland, 2013a.
930 United Nations Environment Programme (UNEP): Minamata Convention on Mercury,
931 available at:

http://www.mercuryconvention.org/Convention/tabid/3426/Default.aspx (last access: 1 February 2016), 2013b.

Verein deutscher Zementwerke e.V. (VDZ): Activity Report 1999–2001, Düsseldorf, Germany, 2002.

Walcek, C., de Santis, S., and Gentile, T.: Preparation of mercury emissions inventory for eastern North America, Environ. Pollut., 123, 375–381, 2003.

Wang, F. Y., Wang, S. X., Zhang, L., Yang, H., Wu, Q. R., and Hao, J. M.: Mercury enrichment and its effects on atmospheric emissions in cement plants of China, Atmos. Environ., 92, 421–428, 2014.

Wang, F. Y., Wang, S. X., Meng, Y., Zhang, L., Wu, Q. R., and Hao, J. M.: Mechanisms and roles of fly ash compositions on the adsorption and oxidation of mercury in flue gas from coal combustion, Fuel, 163, 232–239, 2016a.

Wang, F. Y., Wang, S. X., Zhang, L., Yang, H., Gao, W., Wu, Q. R., and Hao, J. M.: Mercury mass flow in iron and steel production process and its implications for mercury emission control, J. Environ. Sci., in press, 2016b.

Wang, L., Wang, S. X., Zhang, L., Wang, Y. X., Zhang, Y. X., Nielsen, C., McElroy, M. B., and Hao, J. M.: Source apportionment of atmospheric mercury pollution in China using the GEOS-Chem model, Environ. Pollut., 190, 166–175, 2014.

Wang, Q. W.: New technology for treatment of mercury-containing acidic wastewater from gas washing process in lead and zinc smelting by biologics, Ph.D. thesis, Central South University, Changsha, China, 2011.

Wang, S. X., Zhang, L., Li, G. H., Wu, Y., Hao, J. M., Pirrone, N., Sprovieri, F., and Ancora, M. P.: Mercury emission and speciation of coal-fired power plants in China, Atmos. Chem. Phys., 10(3), 1183–1192, 2010a.

Wang, S. X., Song, J. X., Li, G. H., Wu, Y., Zhang, L., Wan, Q., Streets, D. G., and Chin, C. K.: Estimating mercury emissions from a zinc smelter in relation to China's mercury control policies, Environ. Pollut., 158(10), 3347–3353, 2010b.

Wang, S. X., Zhang, L., Hao, J. M., Chen, J. B., Li, Z. G., Yan, N. Q., and Qu, Z.: Mid-term Report for Emission Inventory and Isotopic Characteristics of Mercury from Anthropogenic Sources in China, Mid-term Seminar for 973 Project "The

962 Pollution Characteristics, Environmental Processes and Emission Control
963 Principle of Mercury in China", Guiyang, China, 2014.
964 Wang, Y., Duan, Y., Yang, L., and Jiang, Y.: An analysis of the factors exercising an
965 influence on the morphological transformation of mercury in the flue gas of a 600
966 MW coal-fired power plant, J. Eng. Therm. Energ. Power, 23(4), 399–403, 2008.
967 Wang, Y., Duan, Y., Yang, L., Zhao, C., Shen, X., Zhang, M., Zhuo, Y., and Chen, C.:
968 Experimental study on mercury transformation and removal in coal-fired boiler
969 flue gases, Fuel Process. Technol., 90(5), 643–651, 2009.
970 Wei, W.: Emission of mercury from biomass fuels burning in rural China, M.S. thesis,
971 Peking University, Beijing, China, 2012.
972 Widmer, N. C., West, J., and Cole, J. A.: Thermochemical study of mercury oxidation
973 in utility boiler flue gases, The 93rd Air and Waste Management Association
974 Annual Meeting, 18–22 June 2000, Salt Lake City, UT, USA, 2000.
975 Wilcox, J., Robles, J., Marsden, D. C. J., and Blowers, P.: Theoretically predicted rate
976 constants for mercury oxidation by hydrogen chloride in coal combustion flue
977 gases, Environ. Sci. Technol., 37, 4199–4204, 2003.
978 Winberg, S., Winthum, J., Tseng, S., and Locke, J.: Evaluation of mercury emissions
979 from coal-fired facilities with SCR-FGD systems, DOE/NETL Mercury Control
980 Technology R&D Program Review, Pittsburgh, PA, USA, 2004.
981 Wo, J., Zhang, M., Cheng, X., Zhong, X., Xu, J., and Xu, X.: Hg2+ reduction and re-
982 emission from simulated wet flue gas desulfurization liquors, J. Hazard. Mater.,
983 172, 1106–1110, 2009.
984 Won, J. H., and Lee, T. G.: Estimation of total annual mercury emissions from cement
985 manufacturing facilities in Korea, Atmos. Environ., 62, 265–271, 2012.
986 Wu, Q. R., Wang, S. X., Zhang, L., Song, J. X., Yang, H., and Meng, Y.: Update of
987 mercury emissions from China's primary zinc, lead and copper smelters, 2000–
988 2010, Atmos. Chem. Phys., 12, 11153–11163, 2012.
989 Wu, Q. R., Wang, S. X., Hui, M. L., Wang, F. Y., Zhang, L., Duan, L., and Luo, Y.: New
990 insight into atmospheric mercury emissions from zinc smelters using mass flow
991 analysis, Environ. Sci. Technol., 49(6), 3532-3539, 2015.

992 Wu, Y., Wang, S. X., Streets, D. G., Hao, J. M., Chan, M., and Jiang, J. K.: Trends in
993 anthropogenic mercury emissions in China from 1995 to 2003, Environ. Sci.
994 Technol., 40(17), 5312–5318, 2006.
995 Yang, X., Duan, Y., Jiang, Y., and Yang, L.: Research on mercury form distribution in
996 flue gas and fly ash of coal-fired boiler, Coal Sci. Technol., 35(12), 55–58, 2007.
997 Yang, M.: Research on atmospheric mercury emission inventory and control technology
998 of gold production in China, Postdoctoral work report, Tsinghua University,
999 Beijing, China, 2015.
1000 Yokoyama, T., Asakura, K., Matsuda, H., Ito, S., and Noda, N.: Mercury emissions from
1001 a coal-fired power plant in Japan, Sci. Total Environ., 259(1–3), 97–103, 2000.
1002 Zhang, H., He, P. J., and Shao, L. M.: Fate of heavy metals during municipal solid waste
1003 incineration in Shanghai, J. Hazard. Mater., 156(1), 365–373, 2008.
1004 Zhang, L.: Emission characteristics and synergistic control strategies of atmospheric
1005 mercury from coal combustion in China, Ph.D. thesis, Tsinghua University,
1006 Beijing, China, 2012.
1007 Zhang, L., Wang, S. X., Meng, Y., and Hao, J. M.: Influence of mercury and chlorine
1008 content of coal on mercury emissions from coal-fired power plants in China,
1009 Environ. Sci. Technol., 46(11), 6385–6392, 2012a.
1010 Zhang, L., Wang, S. X., Wu, Q. R., Meng, Y., Yang, H., Wang, F. Y., and Hao, J. M.:
1011 Were mercury emission factors for Chinese non-ferrous metal smelters
1012 overestimated? Evidence from onsite measurements in six smelters, Environ.
1013 Pollut., 171, 109–117, 2012b.
1014 Zhang, L., Daukoru, M., Torkamani, S., Wang, S. X., Hao, J. M., and Biswas, P.:
1015 Measurements of mercury speciation and fine particle size distribution on
1016 combustion of China coal seams, Fuel, 104, 732–738, 2013a.
1017 Zhang, L., Wang, S. X., Wang, F. Y., Yang, H., Wu, Q. R., and Hao, J. M.: Mercury
1018 transformation and removal in three coal-fired power plants with selective
1019 catalytic reduction systems, The 11th International Conference on Mercury as a
1020 Global Pollutant, 28 July–2 August 2013, Edinburgh, Scotland, UK, 2013b.
1021 Zhang, L., Wang, S. X., Wang, L., Wu, Y., Duan, L., Wu, Q. R., Wang, F. Y., Yang, M.,

Yang, H., Hao, J. M., and Liu, X.: Updated emission inventories for speciated atmospheric mercury from anthropogenic sources in China, Environ. Sci. Technol., 49(5), 3185–3194, 2015.

Zhang, W., Wei, W., Hu, D., Zhu, Y., and Wang, X. J.: Emission of speciated mercury from residential biomass fuel combustion in China, Energ. Fuel., 27(11), 6792–6800, 2013.

Zheng, Y., Jensen, A. D., Windelin, C., and Jensen, F.: Review of technologies for mercury removal from flue gas from cement production processes, Prog. Energ. Combust. Sci., 38, 599–629, 2012.

Zhou, J., Wang, G., Luo, Z., and Cen, K.: An experimental study of mercury emissions from a 600 MW pulverized coal-fired boiler, J. Eng. Therm. Energ. Power, 21(6), 569–572, 2006.

Zhou, J., Zhang, L., Luo, Z., and Hu, C.: Study on mercury emission and its control for boiler of 300 MW unit, Therm. Power Gener., 37(4), 22–27, 2008.

**Table 1. Average speciation profiles (ranges) of mercury emissions from coal combustion by boiler type and control technology (%)**

| No. | Boiler type | APCD combination | $Hg^0$ | $Hg^{2+}$ | $Hg_p$ | No. of tests |
|---|---|---|---|---|---|---|
| 1 | PC/SF | None | 56 (8-94) | 34 (5-82) | 10 (1-28) | 13 |
| 2 | SF | WS | 65 (39-87) | 33 (10-60) | 2.0 (0.2-4.5) | 6 |
| 3 | PC | ESP | 58 (16-95) | 41 (5-84) | 1.3 (0.1-10) | 31 |
| 4 | PC | ESP+WFGD | 84 (74-96) | 16 (4-25) | 0.6 (0.1-1.9) | 7 |
| 5 | PC | SCR+ESP+WFGD | 74 (16-96) | 26 (4-84) | 0.2 (0.1-0.4) | 6 |
| 6 | PC | FF | 50 (25-63) | 49 (36-75) | 0.5 (0.1-1.0) | 3 |
| 7 | PC | FF+WFGD | 78 | 21 | 0.9 | 1 |
| 8 | CFB | ESP | 72 | 27 | 0.6 | 1 |

Notes: PC boiler – pulverized-coal boiler; SF boiler – stoker-fired boiler; CFB boiler – circulating fluidized bed boiler; WS – wet scrubber; ESP – electrostatic precipitator; FF – fabric filter; WFGD – wet flue gas desulfurization; SCR – selective catalytic reduction. References to Table 1 are listed in Section 2.3.

**Table 2. Average speciation profiles of mercury emissions from non-ferrous metal smelters by control technology (%)**

| Metal type | APCD combinations | $Hg^0$ | $Hg^{2+}$ | $Hg_p$ | Reference |
|---|---|---|---|---|---|
| Non-ferrous metal | N.S. | 80 | 15 | 5 | Streets et al. (2005)<br>Pacyna et al. (2006)<br>Wu et al. (2006) |
| Zinc | DC+ PS + MRT + $AP_d$ | 71 | 28 | 1 | Wu et al. (2015) |
| Zinc | DC+ PS + $AP_d$ | 55 | 44 | 1 | Zhang et al. (2012b)<br>Wu et al. (2015) |
| Lead | DC+PS+ $AP_s$ | 40 | 60 | 0 | Zhang et al. (2012b) |
| | DC+ PS + $AP_d$ | 39 | 61 | 0 | Zhang et al. (2012b) |
| Copper | DC + PS + $AP_d$ | 50 | 50 | 0 | Zhang et al. (2012b) |
| Gold | DC + PS + $AP_d$ | 32 | 57 | 11 | Yang (2015) |

Notes: N.S. – not specific; DC – dust collector; PS – purification system; MRT – mercury reclaiming tower; $AP_d$ – acid plant with double-conversion-double-absorption processes; $AP_s$ – acid plant with single-conversion-single-absorption processes.

**Table 3. Average proportions of emitted mercury species from cement clinker production (%)**

| Production processes | $Hg^0$ | $Hg^{2+}$ | $Hg_p$ | References |
|---|---|---|---|---|
| N.S. | 80 | 15 | 5 | Streets et al.(2005) |
| N.S. | 85 | 15 | 0 | Won and Lee(2012) |
| Precalciner process (raw mill off) | 16.0 | 75.7 | 8.3 | Mlakar et al. (2010) |
| Precalciner process (raw mill on) | 43.1 | 45.5 | 11.4 | Mlakar et al. (2010) |
| Precalciner process | 9.2 | 90.8 | 0.0 | F. Y. Wang et al. (2014) |
| Precalciner process | 38.7 | 61.3 | 0.0 | F. Y. Wang et al. (2014) |
| Precalciner process | 23.4 | 75.1 | 1.6 | F. Y. Wang et al. (2014) |

Note: N.S. – not specific.

1054 **Table 4. Comparison of sectoral mercury speciation profiles for different countries and regions (%)**

| Countries or regions | Global | | | China | | | South Korea | | | Europe | | | USA | | | Australia | | | New Zealand | | |
|---|---|---|---|---|---|---|---|---|---|---|---|---|---|---|---|---|---|---|---|---|---|
| Inventory year | 2005 | | | 2010 | | | 2007 | | | 2000 | | | 2005 | | | 2006 | | | 2008 | | |
| Mercury emission source | $Hg^0$ | $Hg^{2+}$ | $Hg_p$ | $Hg^0$ | $Hg^{2+}$ | $Hg_p$ | $Hg^0$ | $Hg^{2+}$ | $Hg_p$ | $Hg^0$ | $Hg^{2+}$ | $Hg_p$ | $Hg^0$ | $Hg^{2+}$ | $Hg_p$ | $Hg^0$ | $Hg^{2+}$ | $Hg_p$ | $Hg^0$ | $Hg^{2+}$ | $Hg_p$ |
| Coal-fired power plants | 50 | 40 | 10 | 79 | 21 | 0 | 47 | 46 | 7 | 50 | 40 | 10 | 57 | 40 | 4 | 77 | 17 | 6 | 50 | 40 | 10 |
| Industrial coal combustion | 50 | 40 | 10 | 66 | 32 | 2 | | | | 50 | 40 | 10 | | | | | | | 50 | 40 | 10 |
| Residential coal combustion | 50 | 40 | 10 | 82 | 17 | 1 | | | | 50 | 40 | 10 | | | | | | | 50 | 40 | 10 |
| Stationary oil combustion | 50 | 50 | 0 | 50 | 40 | 10 | 23 | 10 | 68 | 50 | 50 | 0 | 61 | 28 | 12 | 77 | 17 | 6 | | | |
| Mobile oil combustion | 50 | 50 | 0 | 50 | 40 | 10 | 87 | 13 | 0 | 50 | 50 | 0 | 61 | 28 | 12 | 77 | 17 | 6 | | | |
| Biomass fuel combustion | 80 | 15 | 5 | 74 | 5 | 21 | | | | | | | | | | | | | | | |
| Municipal solid waste incineration | 20 | 60 | 20 | 96 | 0 | 4 | 36 | 61 | 3 | 25 | 58 | 17 | 61 | 28 | 12 | 77 | 17 | 6 | | | |
| Cremation | 80 | 15 | 5 | 96 | 0 | 4 | 65 | 12 | 23 | | | | | | | 80 | 10 | 10 | | | |
| Zinc smelting | 80 | 15 | 5 | 30 | 65 | 5 | 73 | 11 | 16 | 75 | 13 | 13 | 61 | 26 | 13 | 77 | 17 | 6 | 80 | 15 | 5 |
| Lead smelting | 80 | 15 | 5 | 57 | 38 | 5 | 38 | 8 | 54 | 75 | 13 | 13 | 61 | 26 | 13 | 77 | 17 | 6 | 80 | 15 | 5 |
| Copper smelting | 80 | 15 | 5 | 47 | 48 | 5 | 28 | 38 | 34 | 75 | 13 | 13 | 61 | 26 | 13 | 77 | 17 | 6 | 80 | 15 | 5 |
| Large-scale gold production | 80 | 15 | 5 | 80 | 15 | 5 | | | | | | | | | | 77 | 17 | 6 | | | |
| Artisanal and small-scale gold mining | 100 | 0 | 0 | 80 | 15 | 5 | | | | | | | | | | | | | | | |
| Mercury production | 80 | 20 | 0 | 80 | 15 | 5 | | | | | | | | | | | | | | | |
| Cement production | 80 | 15 | 5 | 34 | 65 | 1 | 83 | 16 | 1 | 80 | 17 | 3 | | | | 77 | 17 | 6 | 80 | 15 | 5 |
| Iron and steel production | 80 | 15 | 5 | 34 | 66 | 0 | 15 | 80 | 5 | 83 | 17 | 0 | 80 | 10 | 9 | 77 | 17 | 6 | 80 | 15 | 5 |
| Chlor-alkali production | 70 | 30 | 0 | 100 | 0 | 0 | | | | 70 | 30 | 0 | | | | 77 | 17 | 6 | | | |
| References | AMAP/UNEP (2008) Pacyna et al. (2006) | | | Zhang et al. (2015) | | | Kim et al. (2010b) | | | Pacyna et al. (2006) | | | Lin et al. (2012) | | | Nelson et al. (2012) | | | Chrystall and Rumsby (2009) | | |

1055

1056 **Figure Captions**

1057 **Fig. 1. Mercury transformation and removal across APCDs in coal-fired power**
1058 **plants.**

1059 **Fig. 2. Mercury transformation and removal in roasting/smelting flue gas.**

1060 **Fig. 3. Mercury speciation after APCDs for non-ferrous metal smelters.**

1061 **Fig. 4. Mercury transformation in the precalciner cement production process.**

1062

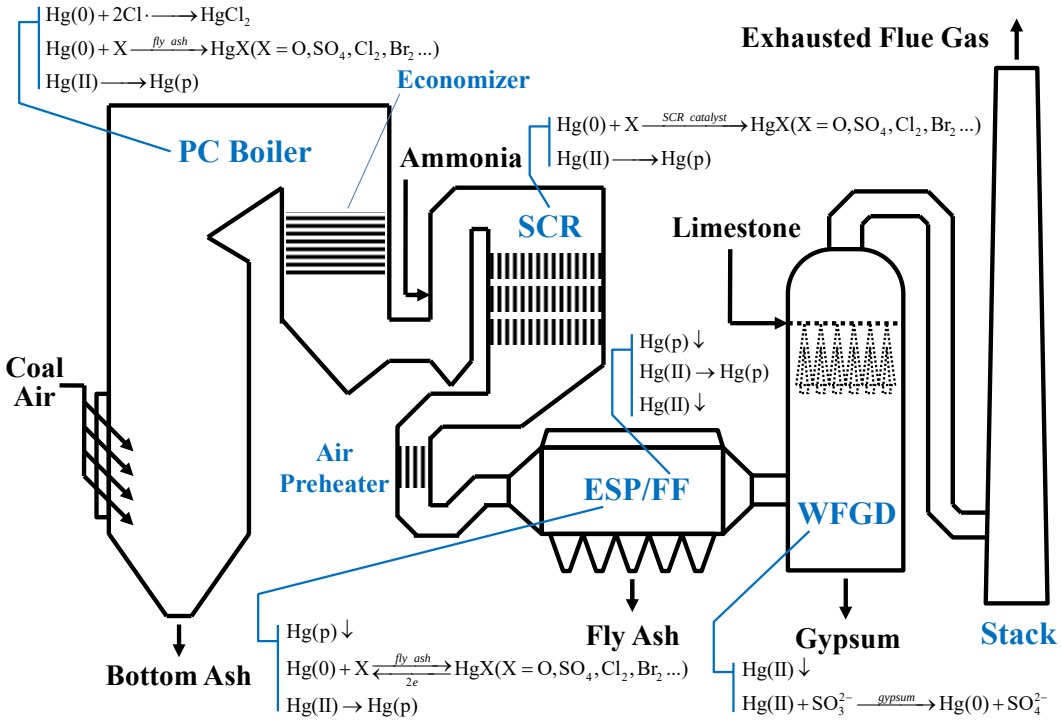


1063

1064 **Fig. 1. Mercury transformation and removal across APCDs in coal-fired power**
1065 **plants.**

1066

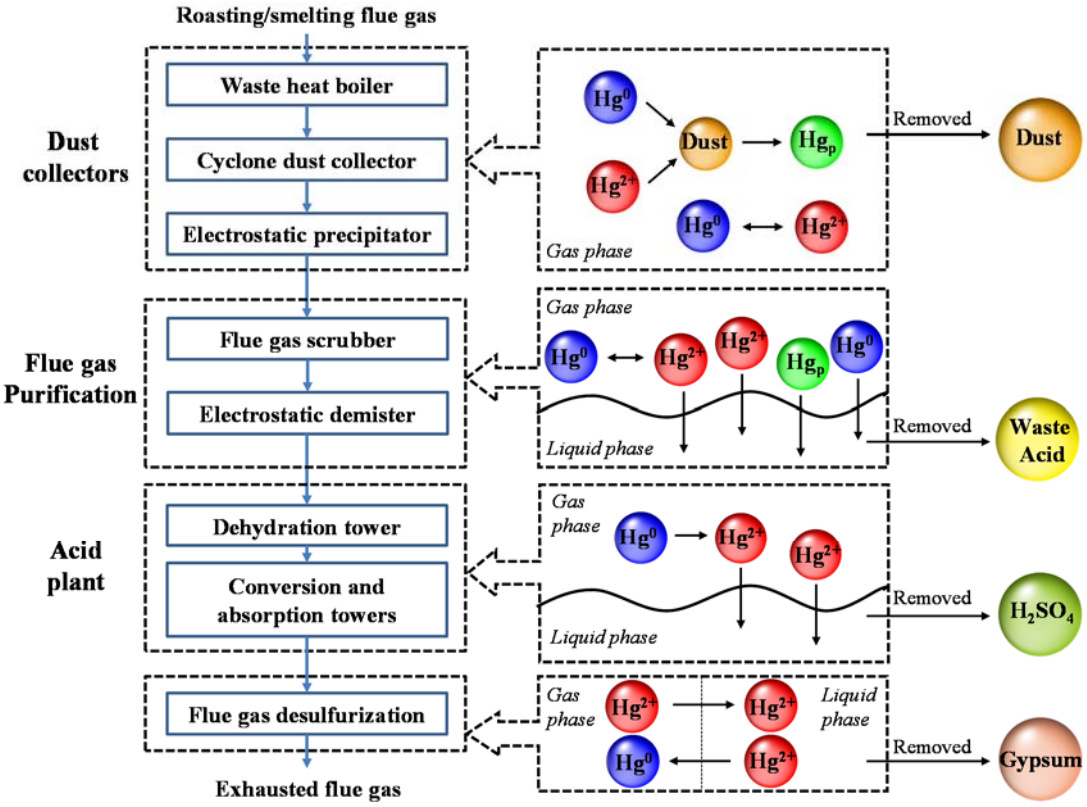


1067

1068 **Fig. 2. Mercury transformation and removal in roasting/smelting flue gas.**

1069

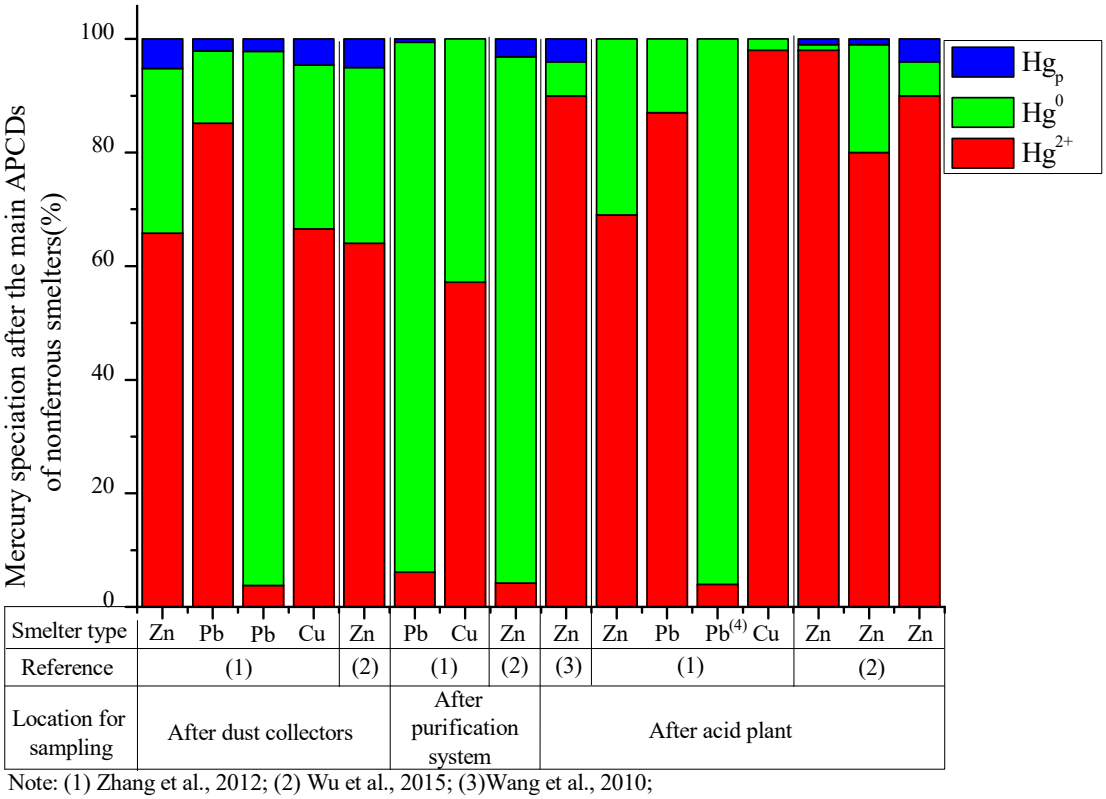


Note: (1) Zhang et al., 2012; (2) Wu et al., 2015; (3)Wang et al., 2010;
(4) Acid plant with single contact and single absorption tower.

**Fig. 3. Mercury speciation after APCDs for non-ferrous metal smelters.**

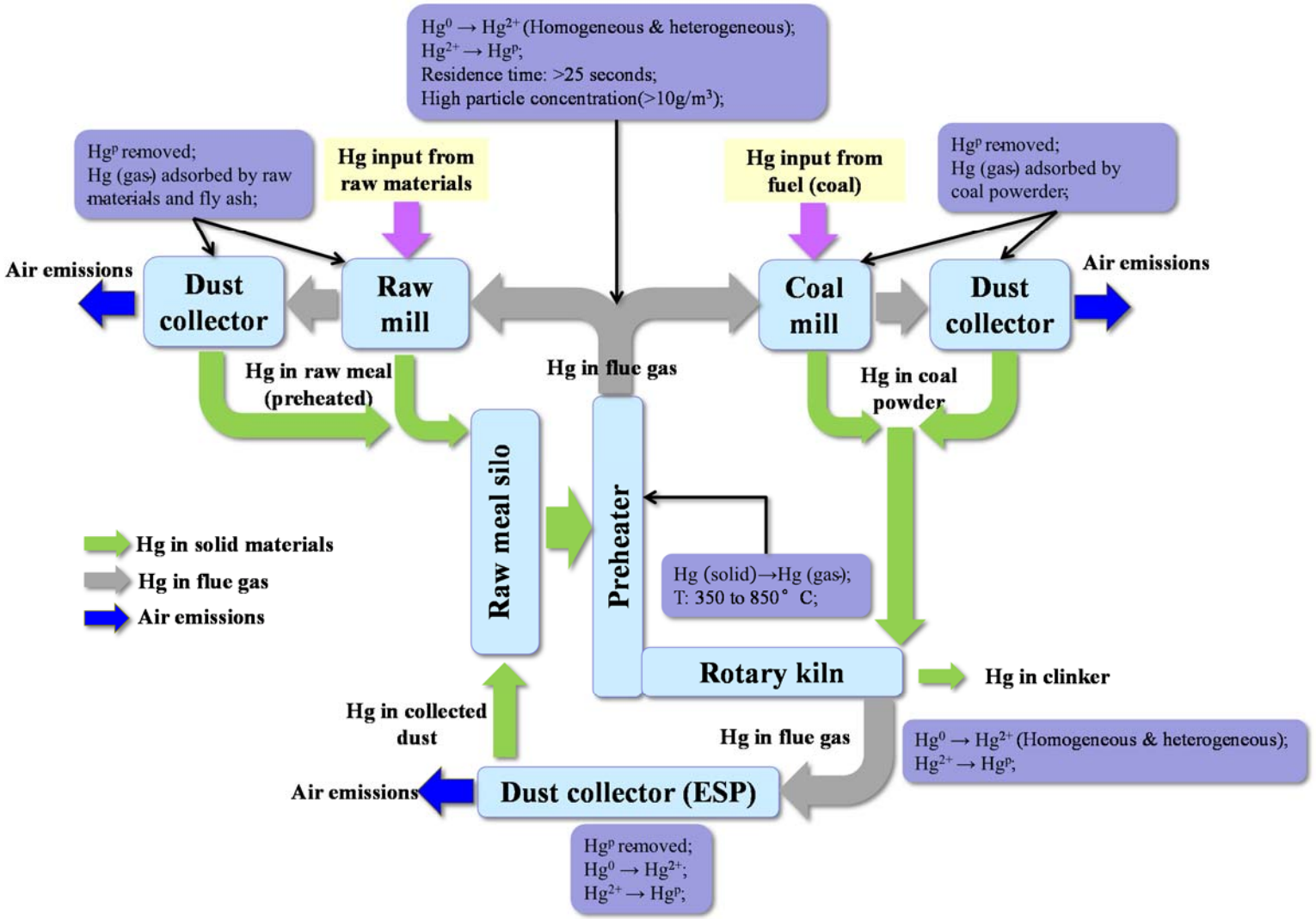


1073

1074 **Fig. 4. Mercury transformation and flow in the precalciner cement production process.**

1075